Inorganic Chemistry

ARTICLE

pubs.acs.org/IC

Construction of Halide-Bridged Tungsten-Copper-Sulfide Double Cubanelike Clusters from a New Precursor $[(Tp^*WS_2)_2(\mu\text{-}S_2)]$

Li-Pei Wei,[†] Zhi-Gang Ren,[†] Lian-Wen Zhu,[†] Wen-Yan Yan,[†] Sha Sun,[†] Hui-Fang Wang,[†] Jian-Ping Lang,[*,†,‡] and Zhen-Rong Sun[*,§]

[†]Key Laboratory of Organic Synthesis of Jiangsu Province, College of Chemistry, Chemical Engineering and Materials Science, Soochow University, Suzhou 215123, People's Republic of China

[‡]State Key Laboratory of Organometallic Chemistry, Shanghai Institute of Organic Chemistry, Chinese Academy of Sciences, Shanghai 200032, People's Republic of China

[§]Department of Physics, East China Normal University, Shanghai 200062, People's Republic of China

Supporting Information

ABSTRACT: Treatment of $[Et_4N][Tp^*WS_3]$ (**1**) (Tp^* = hydridotris(3,5-dimethylpyrazol-1-yl)borate) with 2 equiv of AgSCN in MeCN afforded a novel neutral compound $[(Tp^*WS_2)_2(\mu\text{-}S_2)]$ (**2**). Reactions of **2** with excess CuX (X = Cl, Br, I) in MeCN and CH_2Cl_2 or $CHCl_3$ formed three neutral W/Cu/S clusters $[\{Tp^*W(\mu_3\text{-}S)_3Cu_3(\mu\text{-}Cl)\}_2Cu(\mu\text{-}Cl)_2(\mu_7\text{-}Cl)(MeCN)]_2$ (**3**), $[\{Tp^*W(\mu_3\text{-}S)_3Cu_3\}_2Br(\mu\text{-}Br)_2(\mu_4\text{-}Br)(MeCN)]$ (**4**), and $[\{Tp^*W(\mu_3\text{-}S)_3Cu_3\}_2\{Cu_2(\mu\text{-}I)_4(\mu_3\text{-}I)_2\}]$ (**5**), respectively. On the other hand, treatment of **2** with CuX (X = Cl, Br) in the presence of Et_4NX (X = Cl, Br) produced two anionic W/Cu/S clusters $[Et_4N][\{Tp^*W(\mu_3\text{-}S)_3Cu_3X\}_2(\mu\text{-}X)_2(\mu_4\text{-}X)]$ (**6**: X = Cl; **7** X = Br). Compounds **2**−**7** were characterized by elemental analysis, IR, UV−vis, ^1H NMR, electrospray ionization (ESI) mass spectra, and single-crystal X-ray crystallography. The dimeric structure of **2** can be viewed as two $[Tp^*WS_2]$ fragments in which two W atoms are connected by one S_2^{2-} dianion. Compounds **3**−**7** all possess unique halide-bridged double cubanelike frameworks. For **3**, two $[Tp^*W(\mu_3\text{-}S)_3Cu_3]^{2+}$ dications are linked via a μ_7-Cl^- bridge, two μ-Cl^- bridges, and a $[Cu(MeCN)(\mu\text{-}Cl)_2]^+$ bridge. For **4**, one $[Tp^*W(\mu_3\text{-}S)_3Cu_3(MeCN)]^{2+}$ dication and one $[Tp^*W(\mu_3\text{-}S)_3Cu_3Br]^+$ cation are linked via a μ_4-Br^- and two μ-Br^- bridges. For **5**, the two $[Tp^*W(\mu_3\text{-}S)_3Cu_3]^{2+}$ dications are bridged by a linear $[(\mu\text{-}I)_2Cu(\mu_3\text{-}I)_2Cu(\mu\text{-}I)_2]^{4+}$ species. For **6** and **7**, two $[Tp^*W(\mu_3\text{-}S)_3Cu_3X]^+$ cations are linked by a μ_4-X^- and two μ-X^- bridges (X = Cl, Br). In addition, the third-order nonlinear optical (NLO) properties of **2**−**7** in $MeCN/CH_2Cl_2$ were investigated by using femtosecond degenerate four-wave mixing (DFWM) technique.

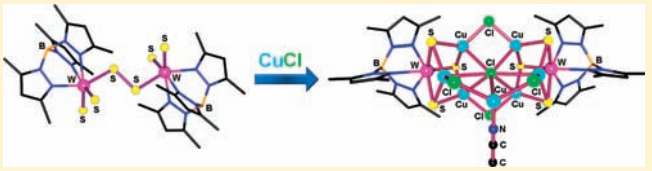

INTRODUCTION

The chemistry of metal sulfide clusters with double cubanelike frameworks has been extensively investigated owing to their geometrical relevance to the active site structures of the P-cluster (Fe_8S_9) and FeMo-cofactor cluster ($MoFe_7S_9$) of nitrogenases,[1,2] their diverse structural chemistry,[3−10] and potential applications in industrial catalytic systems[11] and optoelectronic materials.[7c,12] Several general synthetic strategies have been developed to prepare those double cubanelike clusters. One is the fragment condensation of the preformed single cubanelike clusters with suitable inorganic and/or organic linkers.[9e] For instance, treatment of single cubanelike cluster $[Et_4N]_2[(Meida)MoFe_3S_4Cl_3]$ with Li_2S or NaOEt/H_2O/Me_2SO yielded sulfido- or oxo-bridged double cubanelike Mo/Fe/S clusters $\{[(Meida)MoFe_3S_4Cl_2]_2(\mu\text{-}S)\}^{4-}$[8,9a,9b] and $\{[(Meida)MoFe_3S_4Cl_2]_2(\mu\text{-}O)\}^{4-}$[8,9a−9c] Another is the so-called self-assembly of mononuclear metal sulfide synthons ($[MS_4]^{2-}$, $[(\eta^5\text{-}C_5Me_5)MS_3]^-$ (M = Mo, W)), metal salts ($FeCl_3$, CuCl, etc.) and suitable ligands (RS^-, S^{2-}, etc.) in organic solvents.[9e] For example, reactions of $[MoS_4]^{2-}$ with $FeCl_3$ and NaSR in methanol gave rise to a number of double cubanelike Mo/Fe/S clusters such as $[Mo_2Fe_6S_8(SR)_9]^{3-}$,[5a] $[Mo_2Fe_6S_8(OMe)_3(SR)_6]^{3-}$,[5b] and so forth. However, in this strategy, there are only a few examples involved in using dinuclear metal sulfide synthons for the formation of Mo(W)/Cu/S double cubanelike clusters.[7c]

In the past decade, we have been interested in the preparations of Mo(W)/Cu(Ag)/S clusters from the mononuclear and binuclear metal sulfide synthons such as $[ME_xS_{4-x}]^{2-}$ (M = Mo, W; E = O, S; x = 0−3), $[(\eta^5\text{-}C_5Me_5)MS_3]^-$ (M = Mo, W), $[(\eta^5\text{-}C_5Me_5)_2Mo_2S_2(\mu\text{-}S)_2]$ and $[Tp^*MS_3]^-$ (Tp^* = hydridotris(3,5-dimethylpyrazol-1-yl)borate, M = Mo, W) in pursuit of new cluster chemistry and new functional materials with third-order nonlinear optical (NLO) properties.[6d,7c,7d,8a,8c,12b,13,14] A series of double cubanelike Mo(W)/Cu/S clusters such as $[PPh_4]_2[(\eta^5\text{-}C_5Me_5)MS_3(CuX)_3]_2$ (M = W, X = Cl;[8a] M = W, X = Br,[8a] M = Mo, X = Br,[8a] M = W, X = CN[6d]), $[(\eta^5\text{-}C_5Me_5)_2Mo_2(\mu_3\text{-}S)_3SCu_2X(\mu\text{-}X)]_2$ (X = Cl, Br, SCN)[7c] and $[\{Tp^*W(\mu_3\text{-}S)_3(CuBr)_3\}(\mu_6\text{-}Br)\{Tp^*W(\mu_3\text{-}S)_3Cu_3(ani)_3\}]$[7d] have been isolated

Received: January 22, 2011
Published: April 08, 2011

Scheme 1. Formation of 2 from Reactions of 1 with AgSCN and Reactions of 2 with CuX (X = Cl, Br, I) or Their Combinations Plus Et_4NX (X = Cl, Br)

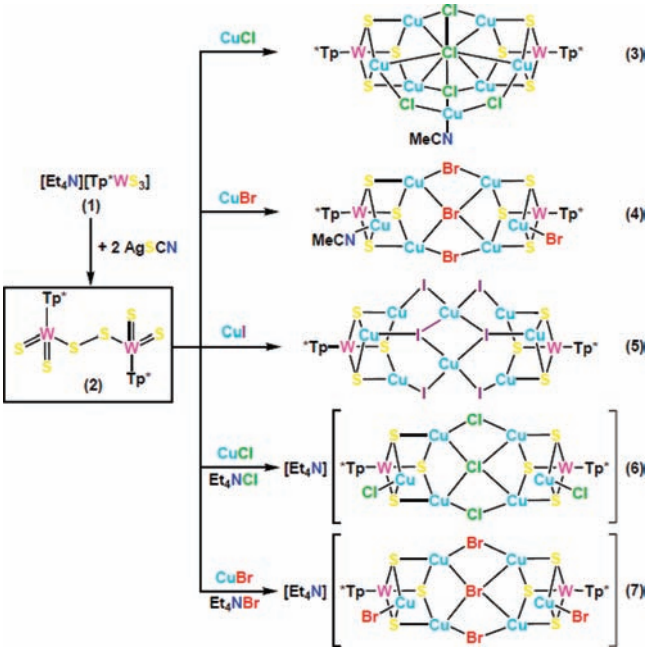

from the aforementioned synthons. Relative to the rich chemistry of the Mo(W)/Cu(Ag)/S clusters derived from $[ME_xS_{4-x}]^{2-}$ (M = Mo, W; E = O, S; x = 0−3) and $[(\eta^5\text{-}C_5Me_5)MS_3]^-$ (M = Mo, W),[7,8,13−15] those originated from $[Tp^*MS_3]^-$ (M = Mo, W) have been less explored.[7d,14e,15a] No Mo(W)/Ag/S clusters derived from this synthon have been reported yet. We thus attempted the reaction of $[Et_4N][Tp^*WS_3]$[15a] (**1**) with AgSCN in MeCN. However, it did not produce any desirable W/Ag/S clusters, but afforded an unexpected neutral dinuclear compound $[(Tp^*WS_2)_2(\mu\text{-}S_2)]$ (**2**). As discussed later in this paper, the molecular structure of **2** possesses two $[Tp^*WS_2]$ fragments linked by one S−S bond, which attracted our attention. It is known that both the oxidative formation and the reductive cleavage of the disulfide bond have been explored as an attractive route to functional sulfide ligands and new materials.[16a−c] For example, reactions involving the cleavage of the S−S bond of 4,4′-dithiodipyridine (dtdp) or 4,4′-dipyridyl disulfide (dpds) with CuI gave rise to Cu/I cluster-based coordination networks such as $[Cu_4I_4(tdp)_2]$ (tdp = 4,4′-thiodipyridine)[16d] and $[Cu_6(\mu\text{-}4\text{-}SpyH)_4I_6]_n$ (4-SpyH = pyridium-4-thiolate).[16e] We anticipated that if the S−S bond of **2** is broken into two $[Tp^*WS_3]^-$ anions, **2** may be used as a new precursor for the preparation of new W/Cu/S clusters. With these considerations in mind, we carried out reactions of **2** with CuX (X = Cl, Br, I) or their combinations plus Et_4NX (X = Cl, Br). Five halide-bridged W/Cu/S doube cubanelike clusters **2**−**7** were isolated therefrom. These compounds showed unprecedented double cubanelike structures in the chemistry of Mo(W)/Cu/S clusters. In addition, **2**−**7** were also confirmed to exhibit good third-order NLO performances in solution through the femtosecond degenerate four-wave mixing (DFWM) technique with 80 fs pulse width at 800 nm. Herein we describe their isolation, structural characterization, and NLO properties.

RESULTS AND DISCUSSION

Synthetic and Spectral Aspects. Reactions of an acetonitrile solution of **1** with 2 equiv of AgSCN afforded a brown solution and a large amount of black precipitate within minutes. The mixture was stirred for 20 h at room temperature and separated by filtration. The resulting black solid was recrystallized in CH_2Cl_2 and then refiltered to give a dark green solution and a black solid. The solution was layered by Et_2O to produce dark green crystals of **2** in 49% yield (Scheme 1). The black solid was assumed to be Ag particles according to its elemental analysis. On the other hand, slow evaporation of solvents from the above brown solution gradually developed an insoluble brown solid. Its IR spectrum showed a W−S streching vibration at 475 cm^{-1} and a B−H stretching vibration of the Tp* group at 2564 cm^{-1}. Its X-ray fluorescence analysis revealed that it contained W, Ag, and S elements. Its powder X-ray diffraction pattern was quite different from those of **1** and **2** (Supporting Information, Figure S1). We therefore assumed it to be a Tp^*WS_3/Ag polymer. Its very low solubility in common organic solvents precluded our growing its single crystals and thus excluded its further structural characterization. The analogous reactions of **1** with other silver salts such as AgX (X = Cl, Br, I) also gave rise to the same product **2** in relatively low yields. The formation of **2** deserves comments. As discussed later in this article, **2** is composed by two $[Tp^*WS_2]$ units linked by a disulfide S_2^{2-}. Such a disulfide is assumed to be derived from oxidizing two terminal sulfides of two discrete $[Tp^*WS_3]^-$ anions of **1** by Ag^+ ion, which was reduced into Ag particles. Since all manipulations were performed under an argon atmosphere using standard Schlenk-line techniques, oxygen as a possible oxidizing agent was excluded. The use of MeCN was critical for the medium-yield formation of **2** because there may exist a formation competition between **2** and the possible Tp^*WS_3/Ag polymer. In addition, we also attempted to run the same reactions in other solvents such as CH_2Cl_2, $CHCl_3$, DMF, and so forth, but the yield of **2** was much lower than that obtained in MeCN.

As indicated in Scheme 1, the reactions of **2** with CuX were straightforward. Treatment of **2** with excess CuX (X = Cl, Br, I) in MeCN and CH_2Cl_2 or $CHCl_3$ followed by standard workups afforded black crystals of **3** in 90% yield, **4** in 85% yield, or **5** in 84% yield. Analogous reactions of **2** with CuX (X = Cl, Br) in the presence of Et_4NX (X = Cl, Br) produced black crystals of **6** in 63% yield and **7** in 66% yield, respectively. To establish the relationship of **3** and **6**, as well as **4** and **7**, we have carried out reactions of **3** with Et_4NCl in MeCN/CH_2Cl_2 and could not isolate **6**. However, reactions of **4** with Et_4NBr in MeCN/CH_2Cl_2 did form **7** in a medium yield.

As reported in our previous work, the anionic trisulfido complex **1** could be used as a building block for cluster synthesis. For example, reactions of **1** with CuX (X = Cl, Br) could only afford anionic single cubane-like clusters $[Et_4N][Tp^*W(\mu_3\text{-}S)_3(CuX)_3]$.[7d,14e] However, complex **2** is a neutral species and when it reacts with CuX, the absence of the Et_4N^+ cation in the reaction system may demand more Cu^+ ions to balance the negative charge of the anionic clusters, which may result in the formation of neutral clusters even with larger nuclearity. This would be one intriguing advantage of **2** in cluster synthesis. For the reactions in Scheme 1, CuX may act as a reducing agent to cleave the disulfide bond in **2** to S^{2-} that coordinates at the W(VI) center in **3**−**7**. Excess Cu^+ or its solvated species or even cationic cluster species in the system also played the role of

dx.doi.org/10.1021/ic200147d |Inorg. Chem. 2011, 50, 4493–4502

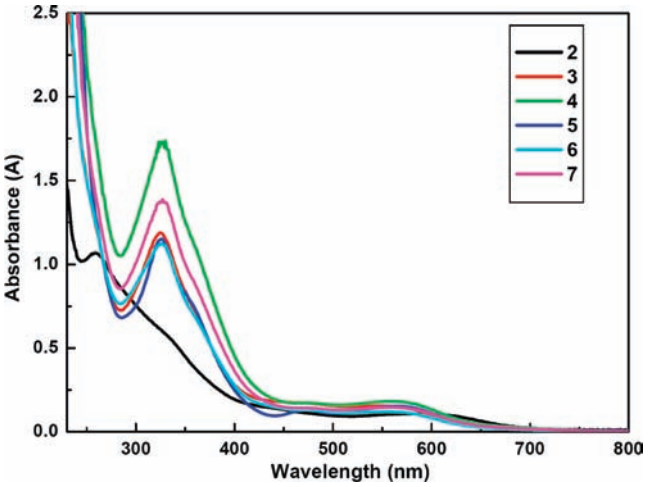

Figure 1. Electronic spectra of **2** (2.7×10^{-5} M), **3** (3.5×10^{-5} M), **4** (7.3×10^{-5} M), **5** (3.0×10^{-5} M), **6** (3.8×10^{-5} M), and **7** (6.4×10^{-5} M) in $MeCN/CH_2Cl_2$ in a 1 cm thick glass cell.

counterpart cation to keep the charge of the resulting anionic clusters balanced. For example, the −1 charge of the $[\{Tp^*W(\mu_3\text{-}S)_3Cu_3\}_2Cl_5]^-$ anion was balanced by addition of a $[Cu(MeCN)]^+$ cation into its cluster framework, thereby forming a neutral cluster **3**. Another example is that the −2 charge of two $[Tp^*W(\mu_3\text{-}S)_3(CuI)_3]^-$ anions of **5** was balanced by incorporation of two Cu^+ ions. Furthermore, the −1 charge of the $[Tp^*W(\mu_3\text{-}S)_3(CuBr)_3]^-$ anion was balanced by the $[Tp^*W(\mu_3\text{-}S)_3Cu_3(MeCN)]^-$ cation to form a neutral cluster of **5**. In the presence of Et_4NX, the formation of the anionic clusters of **6** and **7** were expected probably because the relatively bulky Et_4N^+ cation may match well with the resulting $[\{Tp^*W(\mu_3\text{-}S)_3Cu_3X\}_2(\mu\text{-}X)_2(\mu_4\text{-}X)]^-$ anion, which may facilitate their crystallization from the solution. Complicated redox processes must be in the above reactions, while the formation mechanism of these halide-bridged double cubane-like clusters is yet to be elucidated.

In the IR spectra of **2**−**7**, bands at 2556 (**2**), 2565 (**3**), 2564 (**4**), 2563 (**5**), 2564 (**6**), and 2558 (**7**) cm^{-1} are assigned to be the B−H stretching vibrations of the Tp* groups, while those at about 1543, 1458, 1547, 1549, 1548, and 1543 cm^{-1} are assumed to be the pyrazolyl rings in **2**−**7**. Bands at 488/473 (**2**), 480/405 (**3**), 479/406 (**4**), 475/416 (**5**), 469/426 (**6**), and 468/418 (**7**) cm^{-1} are assigned as the bridging W−S stretching vibrations in **2**−**7**. The ^1H NMR spectra of **2**−**7** in $CDCl_3$ or DMSO-d_6 at room temperature show two singlets with the same intensities at 2.29/2.80 (**2**), 2.35/2.87 (**3**), 2.39/2.86 (**4**), 2.26/2.79 (**5**), 2.38/2.86 (**6**), and 2.36/2.84 (**7**) ppm and one singlet at 6.05 (**2**), 5.99 (**3**), 6.14 (**4**), 6.11 (**5**), 6.09 (**6**), and 6.13 (**7**) ppm, which can be assigned to be the methyl protons and the pyrazolyl methine protons of the Tp* moiety. It is noted that in the crystal structure of **4**, two Tp* ligands are inequivalent as described later in this article. However, it seems that the coordinated acetonitrile and the terminal bromide rapidly exchanged their coordination sites in solution at the NMR time scale, which caused the two Tp* ligands to be equivalent in its ^1H NMR spectroscopy. In addition, one singlet at 2.09 (**3**) and 2.11 (**4**) ppm should be the methyl protons of MeCN in **3** and **4**, while multiplets at 1.12−1.16, 3.20−3.29 (**6**) and 1.15−1.19, 3.14−3.21 (**7**) ppm are assignable to be the ethyl protons of the Et_4N^+ cation. The UV−vis

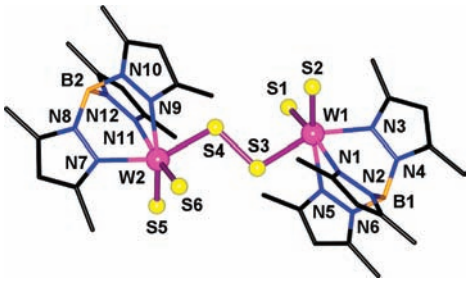

Figure 2. View of the molecular structure of **2** with a labeling scheme. All hydrogen atoms are omitted for clarity. Selected bond lengths (Å): W(1)−S(1) 2.151(2), W(1)−S(2) 2.162(3), W(1)−S(3) 2.391(2), W(2)−S(4) 2.393(2), W(2)−S(5) 2.146(2), W(2)−S(6) 2.145(2), S(3)−S(4) 2.046(3).

spectra of **2**−**7** in $MeCN/CH_2Cl_2$ were characterized by one main band (Figure 1). Relative to the band at 259 nm of **2**, those at 325 (**3**), 326 (**4**−**6**), and 327 (**7**) nm are red-shifted, and they are probably originated from the S→W(VI) charge-transfer transitions of the common Tp^*WS_3 moiety.[7d,14e]

The positive-ion (**3**−**5**) and negative-ion (**6** and **7**) ESI-MS spectra in dimethylformamide (DMF) did not show any parent cationic cluster peaks, but a set of cluster fragment peaks (Supporting Information, Figures S2−S5). For **3**−**5**, they all had two peaks at $m/z = 736.9$ ($[Tp^*WS_4Cu_2]^+$) and $m/z = 829.9$ ($[(Tp^*WS_4Cu_2) + DMF + H_2O + 2H]^+$). These species might be formed by breaking part of the double cubanelike frameworks under the mass conditions. In addition, their ESI mass spectra presented other peaks at $m/z = 1775.5$ ($[(Tp^*WS_3Cu_3)_2Br_3]^+$), $m/z = 1488.8$ ($[(Tp^*WS_3)_2Cu_4Br]^+$), and $m/z = 1344.9$ ($[(Tp^*WS_3)_2Cu_3]^+$) for **4**; $m/z = 1726.5$ ($[(Tp^*WS_3)_2Cu_5I_2]^+$) for **5**; $m/z = 902.8$ ($[(Tp^*WS_3Cu_2Cl_3) + DMF + H_2O + H]^-$) and $m/z = 794.9$ ($[(Tp^*WS_3Cu_2Cl_2) + H_2O]^-$) for **6**. For **7**, the negative ESI mass spectrum was quite messy, and we could not figure out any peaks that match well with their theoretical isotopic patterns.

Crystal Structure of $[(Tp^*WS_2)_2(\mu\text{-}S_2)]$ (2). Crystallized in the monoclinic space group $P2_1/c$, the asymmetric unit of $\mathbf{2}\cdot 2CH_2Cl_2$ contains one discrete $[(Tp^*WS_2)_2(\mu\text{-}S_2)]$ molecule and two CH_2Cl_2 solvent molecules. **2** contains two $[Tp^*WS_2]^+$ fragments bridged by a $\mu\text{-}S_2^{2-}$ anion to form a unique dimeric structure (Figure 2). Each W center was assumed to be a +6 oxidation state and adopts a distorted octahedral coordination geometry, coordinated by three N atoms from a Tp* ligand, two terminal S atoms, and one S atom from $\mu\text{-}S_2$. The mean terminal W═S bond length (2.151(2) Å) (Supporting Information, Table S1) is somewhat shorter than that of **1** (2.194(2) Å)[15a] while the average W−μ-S bond length (2.392(2) Å) is shorter than that of $[(Fulvalene)W_2(\mu\text{-}S_2)(CO)_6]$ (2.492(5) Å, Fulvalene = bicyclopentadienylidene).[17] The S3−S4 bond length of **2** (2.046(3) Å) is shorter than those of the corresponding ones of complexes containing a $\mu\text{-}S_2^{2-}$ bridge such as $[(Fulvalene)W_2(\mu\text{-}S_2)(CO)_6]$ (2.065(6) Å) and $[Et_4N]_2\{W_2O_2(\mu_2\text{-}S)(S_2)_4\}_{0.77}\{W_2O_2(\mu_2\text{-}S_2)(S_2)_4\}_{0.23}$ (2.10(5) Å).[18]

Crystal Structure of $[\{Tp^*W(\mu_3\text{-}S)_3Cu_3(\mu\text{-}Cl)\}_2Cu(\mu\text{-}Cl)_2(\mu_7\text{-}Cl)(MeCN)]$ (3). Compound $\mathbf{3}\cdot CH_2Cl_2$ crystallizes in the orthorhombic space group *Pnma*, and its asymmetric unit contains half a $[\{Tp^*W(\mu_3\text{-}S)_3Cu_3(\mu\text{-}Cl)\}_2Cu(\mu\text{-}Cl)_2(\mu_7\text{-}Cl)(MeCN)]$ molecule and one CH_2Cl_2 solvent molecule. **3** consists of two incomplete cubanelike $[Tp^*W(\mu_3\text{-}S)_3Cu_3]$ fragments that are connected via a μ_7-Cl bridge, two μ-Cl bridges, and a [Cu(MeCN)

dx.doi.org/10.1021/ic200147d |*Inorg. Chem.* 2011, 50, 4493–4502

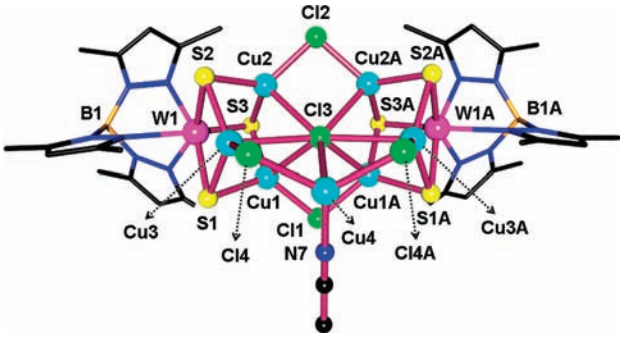

Figure 3. View of the molecular structure of **3** with a labeling scheme. All hydrogen atoms are omitted for clarity. Symmetry code: A: $-x, 1-y, -z$. Selected bond lengths (Å): W···Cu(av.) 2.6618(9), Cu−μ_7-Cl (av.) 2.7112(16) Å, Cu−μ-Cl (av.) 2.2489(16) Å, W−μ_3-S(av.) 2.3095(16), Cu−μ_3-S(av.) 2.2283(16).

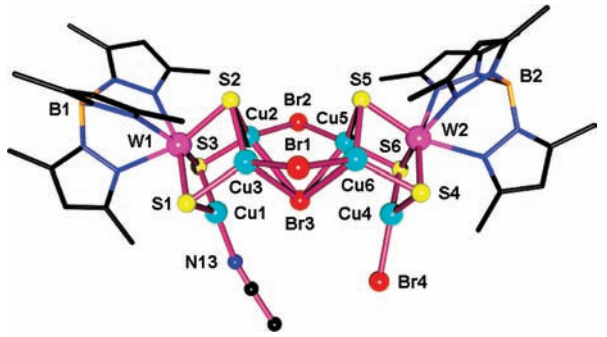

Figure 4. View of the molecular structure of **4** with a labeling scheme. All hydrogen atoms are omitted for clarity. Selected bond lengths (Å): W···Cu(av.) 2.6766(15) Å, Cu−μ_4-Br3 2.8273(18) Å, Cu−μ-Br(av.) 2.3706(17) Å, Cu−Br4 2.3159(17), W−μ_3-S(av.) 2.302, Cu−μ_3-S(av.) 2.233(2), Cu1−N1 1.918(9).

(μ-Cl)$_2$] bridge, forming an uncommon double cubanelike structure (Figure 3). Occurrence of such a combination of three different bridges to link two incomplete cubanelike fragments is unprecedented in the chemistry of $[MS_4]^{2-}$ and $[(\eta^5\text{-}C_5Me_5)MS_3]^-$ (M = Mo, W). There is one crystallographic mirror plane going through Cl1, Cl2, Cl3, Cu4, N7, C16, and C17. The Cu1, Cu2, Cu3 and their symmetry-related ones are tetrahedrally coordinated by a μ-Cl atom, a μ_7-Cl atom, and two μ_3-S atoms while Cu4 is tetrahedrally coordinated by a μ_7-Cl atom, two μ-Cl atoms, and one N atom from one MeCN molecule. The average W···Cu contact (2.6618(9) Å) of **3** (Supporting Information, Table S1) is shorter than those in W/Cu/S clusters containing tetrahedrally coordinated Cu such as $[Tp^*W(\mu_3\text{-}S)_3Cu_3(\mu\text{-}NCS)_3(CuMeCN)]_2$ (2.7193(16) Å),[14e] $[(\eta^5\text{-}C_5Me_5)WS_3Cu]_4$ (2.751(3) Å),[13b] and $[WS_4Cu_4(dppm)_4](PF_6)_2$ (2.760(1) Å).[13a] The mean Cu−μ_7-Cl length (2.7112(16) Å) is quite long, and existence of a μ_7-Cl bridge is quite rare in copper-containing compounds. The Cu−μ-Cl bond length (2.2489(16) Å) in **3** is shorter than those found in $[(\eta^5\text{-}C_5Me_5)_2Mo_2(\mu_3\text{-}S)_3SCu_2Cl(\mu\text{-}Cl)]_2$ (2.3821(13) Å)[7c] and $[PPh_4]_2[(\eta^5\text{-}C_5Me_5)WS_3(CuCl)_3]_2$ (2.461(7) Å).[8a] The mean W−μ_3-S and Cu−μ_3-S bond lengths are normal.

Crystal Structure of $[\{Tp^*W(\mu_3\text{-}S)_3Cu_3\}_2Br(\mu\text{-}Br)_2(\mu_4\text{-}Br)(MeCN)]$ (4). $4\cdot CH_2Cl_2\cdot 2CHCl_3$ crystallizes in the triclinic space group $P\bar{1}$, and its asymmetric unit consists of one discrete $[\{Tp^*W(\mu_3\text{-}S)_3Cu_3\}_2Br(\mu\text{-}Br)_2(\mu_4\text{-}Br)(MeCN)]$ molecule, one CH_2Cl_2 solvent molecule, and two $CHCl_3$ solvent molecules. The double cubanelike structure of **4** may be considered as being built of two incomplete cubanelike fragments, $[Tp^*W(\mu_3\text{-}S)_3Cu_3(MeCN)]$ and $[Tp^*W(\mu_3\text{-}S)_3Cu_3Br]$, which are linked via a μ_4-Br and two μ-Br bridges (Figure 4). Cu2, Cu3, Cu5, and Cu6 centers are tetrahedrally coordinated by a μ-Br atom, a μ_4-Br atom, and two μ_3-S atoms while Cu1 or Cu4 is trigonally coordinated by two μ_3-S atoms and one N atom from MeCN or by one terminal Br and two μ_3-S atoms. The μ_4-Br adopts a rare square pyramidal coordination geometry. For the trigonally coordinated Cu, the average W···Cu contact (2.6571(15) Å) (Supporting Information, Table S1) is slightly longer than that found in the clusters having three-coordinated Cu such as $[Et_4N][Tp^*W(\mu_3\text{-}S)_3(CuCl)_3]$ (2.6404(18) Å).[14e] For the tetrahedrally coordinated Cu, the average W···Cu contact (2.6766(15) Å) is close to that of **3**. The mean Cu−μ_4-Br3 length (2.8273(18) Å) in **4** is longer than that of the corresponding one of $[Cu_2(OH)_2(C_{10}H_8N_2)_2][Cu_4Br_6]$ (2.5774(9) Å).[19a] The Cu−μ-Br bond length (2.3706(17) Å) is shorter than that in $[PPh_4]_2[\{(\eta^5\text{-}C_5Me_5)WS_3\}_2Cu_6Br_6]$ (2.616(1) Å).[6b] The mean W−μ_3-S and Cu−μ_3-S bond lengths are normal.

Crystal Structure of $[\{Tp^*W(\mu_3\text{-}S)_3Cu_3\}_2\{Cu_2(\mu\text{-}I)_4(\mu_3\text{-}I)_2\}]$ (5). Crystallized in the triclinic space group $P\bar{1}$, the asymmetric unit of **5** contains half a $[\{Tp^*W(\mu_3\text{-}S)_3Cu_3\}_2\{Cu_2(\mu\text{-}I)_4(\mu_3\text{-}I)_2\}]$ molecule. In **5**, two incomplete cubanelike $[Tp^*W(\mu_3\text{-}S)_3Cu_3]$ fragments are linked via a $[Cu_2(\mu\text{-}I)_4(\mu_3\text{-}I)_2]$ species to afford an unprecedented double incomplete cubanelike structure with a symmetry center located at the midpoint of Cu4 and Cu4A (Figure 5). Alternatively, this double cubanelike structure may be constructed by placing a $[Cu_2(\mu_3\text{-}I)_2]$ rhomb in-between two incomplete cubanelike $[Tp^*W(\mu_3\text{-}S)_3Cu_3(\mu\text{-}I)_2]$ fragments followed by forming a pair of Cu−μ_3-I bonds and two pairs of Cu−μ-I bonds. Each Cu atom in two $[Tp^*W(\mu_3\text{-}S)_3Cu_3]$ fragments is trigonally coordinated by two μ_3-S atoms and one μ-I atom (Cu1 and Cu3) or one μ_3-I atom (Cu2). In the $[Cu_2(\mu\text{-}I)_4(\mu_3\text{-}I)_2]$ species, each Cu atom is tetrahedrally coordinated by two μ-I atoms and two μ_3-I atoms. The mean W···Cu separation (2.645(3) Å) (Supporting Information, Table S1) is somewhat shorter than those of the corresponding ones of clusters containing trigonally coordinated Cu such as **4** and $[PPh_4]_2[[(\eta^5\text{-}C_5Me_5)WS_3Cu_3Cl_3]_2$ (2.654(3) Å).[8a] For the trigonally coordinated Cu, the average Cu−μ-I and Cu−μ_3-I bond lengths (2.470(3) Å vs 2.460(3) Å) are shorter than those of the corresponding ones of $[\{((\eta^5\text{-}C_5Me_5)Mo)_2As_2S_3\}_3(CuI)_7]$ (2.587(2) Å vs 2.677(2) Å).[19b] For the tetrahedrally coordinated Cu, the average Cu−μ-I and Cu−μ_3-I bond lengths (2.795(5) Å vs 2.938(5) Å) are longer than those in $[Cs_2(18c6)_3][Cu_8I_{10}(MeCN)_2]$ (2.579(2) Å vs 2.705(2) Å, 18c6 = 18-crown-6).[19c] The mean W−μ_3-S and Cu−μ_3-S bond lengths are normal.

It is noted that the structure of **5** is totally different from those of **3** and **4**. Such a difference may be due to the different atomic radii of Cl, Br, and I. The atom radius of Br is larger than that of Cl and existence of a μ_7-Br bridge in the analogous structure of **3** would make the framework too crowed be unstable. Thus such a bromide adopts a relatively low coordination number, that is, a μ_4-Br bridge in **4**. In the case of **5**, the atomic radius of I is much larger than those of Cl and Br atoms, neither a μ_7-I nor a μ_4-I bridge could afford similar structures to **3** and **4**. The iodide atoms in **5** take lower coordination numbers, that is, μ_3-I and μ-I bridges.

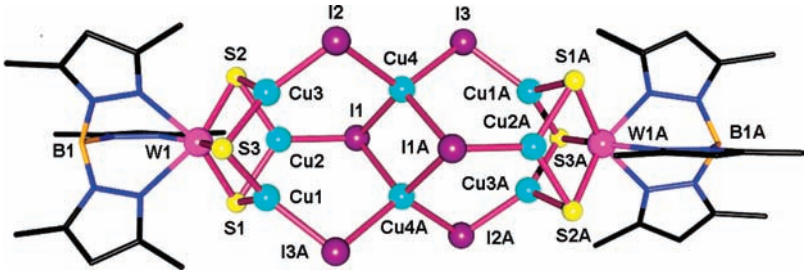

Figure 5. View of the molecular structure of **5** with a labeling scheme. All hydrogen atoms are omitted for clarity. Symmetry code: A: $-x, -y+2, -z+1$. Selected bond lengths (Å): W···Cu(av.) 2.645(3) Å, W–μ_3-S(av.) 2.316(5), Cu–μ_3-S(av.) 2.214(6). For the trigonally coordinated Cu, Cu–μ-I(av.) 2.470(3), Cu–μ_3-I(av.) 2.460(3). For the tetrahedrally coordinated Cu, Cu–μ-I(av.) 2.795(5), Cu–μ_3-I(av.) 2.938(5).

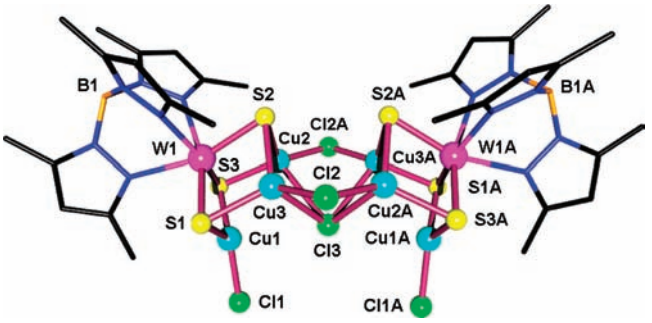

Figure 6. Perspective view of the anion structure of **6** with a labeling scheme. All hydrogen atoms are omitted for clarity. Symmetry code: A: $1-x, -y, -z$. Selected bond lengths (Å): W···Cu(av.) 2.6592(9) Å, Cu1–Cl1 2.1719(18), Cu–μ-Cl(av.) 2.2470(16) Å, Cu–μ_4-Cl3(av.) 2.6945(15) Å, W–μ_3-S(av.) 2.3049(15), Cu–μ_3-S(av.) 2.2291(17).

Crystal Structures of $[Et_4N][\{Tp^*W(\mu_3\text{-}S)_3Cu_3Cl\}_2(\mu\text{-}Cl)_2(\mu_4\text{-}Cl)]$ (6) and $[Et_4N][\{Tp^*W(\mu_3\text{-}S)_3Cu_3Br\}_2(\mu\text{-}Br)_2(\mu_4\text{-}Br)]$ (7). Crystallized in the same orthorhombic space group *Pbcn*, the asymmetric unit for **6**·Et_2O or **7**·$1.5Et_2O$ contains one-half of the $[\{Tp^*W(\mu_3\text{-}S)_3Cu_3Cl\}_2(\mu\text{-}X)_2(\mu_4\text{-}X)]^-$ (X = Cl, Br) anion, half a Et_4N^+ cation, and half a Et_2O solvent molecule (**6**) or one-half and a quarter of Et_2O solvent molecules (**7**). Their cell parameters are essentially identical, as the structures of the anion cluster. Therefore only the perspective view of the $[\{Tp^*W(\mu_3\text{-}S)_3Cu_3Cl\}_2(\mu\text{-}Cl)_2(\mu_4\text{-}Cl)]^-$ anion of **6** is shown in Figure 6. In the anion of **6** or **7**, two incomplete cubanelike $[Tp^*W(\mu_3\text{-}S)_3Cu_3X]$ fragments are connected by a μ_4-X and two μ-X bridges (X = Cl, Br), forming a unique anionic double incomplete cubanelike structure, which closely resemble that of **4**. In each incomplete cubanelike $[Tp^*W(\mu_3\text{-}S)_3Cu_3X]$ fragment, one Cu atom is trigonally coordinated by one terminal X and two μ_3-S atoms while two Cu centers are tetrahedrally coordinated by a μ-X atom, a μ_4-X atom, and two μ_3-S atoms. The μ_4-X also has a similar square pyramidal coordination sphere to that of **4**.

As indicated in the Supporting Information, Table S1, for the trigonally coordinated Cu, the average W···Cu contact in either **6** or **7** is longer than that of the corresponding one of **4**. For the tetrahedrally coordinated Cu, the average W···Cu contact (2.6592(9) Å) in **6** is shorter than those of the corresponding ones of **4** and **7** (2.6735(11) Å). The average Cu–μ-Cl bond length of **6** (2.2470(16) Å) is almost the same as that of **3**. The mean Cu–μ_4-Cl3 length (2.6945(15) Å) in **6** is longer than that in $[Cu_6(dppm)_2(\mu_4\text{-}Cl)\{S_2P(O^iPr)_2\}_4](BF_4)$ (2.6239(18) Å).[19d] For **7**, the mean terminal Cu–Br and Cu–μ-Br bond lengths (2.3123(14) Å vs 2.3775(12) Å) are comparable to those of the corresponding ones of **4**. The mean Cu–μ_4-Br length (2.8070(13) Å) of **7** is slightly shorter than that of **4**. The mean W–μ_3-S and Cu–μ_3-S bond lengths in **6** and **7** are normal.

Third-Order Nonlinear Optical (NLO) Properties of 2–7. As indicated in Figure 1, the UV–vis spectra of **2**–**7** in CH_2Cl_2/MeCN showed almost no linear absorption at 750–800 nm. The laser wavelength (800 nm) employed in the experiment of DFWM was out of the absorption region, which guaranteed low intensity loss and little temperature change by photon absorption during the NLO measurements.[20a,b] Thus the off-resonant third-order optical nonlinearities of **2**–**7** could be measured. The nonlinear absorption performances of **2**–**7** in CH_2Cl_2/MeCN were evaluated by the DFWM technique under an open-aperture configuration. The dependence of time-resolved DFWM signal intensity on the delay time of the input beam is shown in Figure 7 and Supporting Information, Figures S8–S11. The curves were obtained via fitting the time convolution between the autocorrelation function of pulse and the single exponent decline function exp $(t/-T_2)$.

The third-order nonlinear optical susceptibility $\chi^{(3)}$ is measured via a comparison with that of a reference sample CS_2, calculated from the DFWM signal (I), the linear refractive index (n), the sample thickness (L), and absorption correction factor using eq 1:[20b]

$$\chi_s^{(3)} = \left(\frac{I_s}{I_r}\right)^{1/2} \cdot \frac{L_r}{L_s} \cdot \left(\frac{n_s}{n_r}\right)^2 \cdot \frac{\alpha \cdot L \cdot \exp(\alpha L/2)}{1-\exp(-\alpha L)} \cdot \chi_r^{(3)} \quad (1)$$

where the subscripts "s" and "r" represent the parameters for the sample and CS_2. And α is the linear absorption coefficient. The last fraction comes from the sample absorption and equals to 1 while the sample has no absorption around the employed laser wavelength. The values of $\chi_r^{(3)}$ and n_r for CS_2 are 6.7×10^{-14} esu and 1.632, respectively.[21] The third-order nonlinear optical susceptibility $\chi^{(3)}$ for **2**–**7** are calculated by eq 1 to be 2.47×10^{-14} esu (**2**), 3.07×10^{-14} esu (**3**), 2.59×10^{-14} esu (**4**), 2.73×10^{-14} esu (**5**), 2.72×10^{-14} esu (**6**), and 2.94×10^{-14} esu (**7**), respectively. These results showed that **2**–**7** possess relatively good third-order optical nonlinearities.

The third-order nonlinear refractive index n_2 in isotropic media is estimated through eq 2:[20c]

$$n_2(esu) = \frac{12\pi\chi^{(3)}}{n^2} \quad (2)$$

where n is the linear refractive index of the solution. The nonlinear refractive index n_2 values are 4.57×10^{-13} esu (**2**),

dx.doi.org/10.1021/ic200147d |*Inorg. Chem.* 2011, 50, 4493–4502

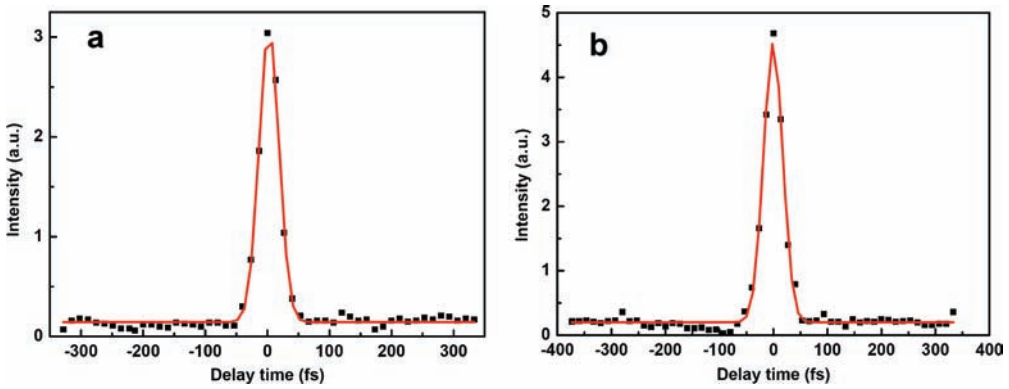

Figure 7. DFWM signal for the CH_2Cl_2/MeCN solutions of 5.0×10^{-5} M for **2** (a) and 5.0×10^{-5} M for **3** (b) with 80 fs laser pulses and 1.5 mm cell. The black solid squares are experimental data, and the red solid curve is the theoretical fit.

5.68×10^{-13} esu (**3**), 4.80×10^{-13} esu (**4**), 5.05×10^{-13} esu (**5**), 5.04×10^{-13} esu (**6**), and 5.44×10^{-13} esu (**7**), respectively.

The second-order hyperpolarizability γ of a molecule in isotropic media is related to the solution $\chi^{(3)}$ by eq 3:[20d]

$$\gamma = \frac{\chi^{(3)}}{Nf^4} \qquad (3)$$

where N is the number density of the solute per milliliter, and f^4 is the local field correction factor which is $[(n^2 + 2)/3]^4$ (n is the linear refractive index of solution). The second-order hyperpolarizability γ values are 1.25×10^{-31} esu (**2**), 3.12×10^{-31} esu (**3**), 2.63×10^{-31} esu (**4**), 2.77×10^{-31} esu (**5**), 2.76×10^{-31} esu (**6**), and 2.98×10^{-31} esu (**7**), respectively. According to eq 3, N represents the number density (concentration) of a compound, and the hyperpolarizability γ value can be used to represent NLO properties of neat materials. It is interesting to compare these new complexes with some other types of complexes including organometallic compounds, semiconductors, and the conjugated polymers previously reported as the promising candidates for NLO materials. When compared with the nanosecond and picosecond measurement values, femtosecond values are roughly 2−3 orders of magnitude lower.[21] The γ values of **3**−**7** are comparable to those found in the well-known conjugated polymers such as Cz-PFE (6.5×10^{-31} esu),[22a] PDEB (9.8×10^{-31} esu),[22b] and TPD-PFE (2.4×10^{-31}),[22c] substituted benzoporphyrin zinc complexes (1.8×10^{-30} esu),[22d] and other M/Cu/S clusters derived from other sulfide synthons $[MS_4]^{2-}$, $[MOS_3]^{2-}$, and $[(\eta^5\text{-}C_5Me_5)MS_3]^-$ (M = Mo, W), such as $[MoS_4Cu_4(\alpha\text{-MePy})_5Br_2]\cdot 2(\alpha\text{-MePy})_{0.5}$ (1.06×10^{-30} esu),[14c] $[(Et_4N)_2\{WS_4Cu_4(CN)_4\}]_n$ (1.26×10^{-29} esu),[23a] $[(n\text{-Bu})_4N]_2[MoOS_3(CuNCS)_3]$ (4.8×10^{-29} esu),[14b] $[WOS_3Cu_3(4\text{-MePy})_6](BF_4)$ (4.43×10^{-31} esu),[23b] $[WOS_3Cu_2(4\text{-}t\text{BuPy})_2]_2$ (4.8×10^{-30} esu),[23c] $\{[((\eta^5\text{-}C_5Me_5)MoS_3Cu_3)_2(\mu\text{-bpp})_3(\mu\text{-NCS})_2(\text{NCS})](\text{NCS})\}_n$ (bpp = 1,3-bis(4-pyridyl)propane, 3.86×10^{-29} esu),[14d] and $[PPh_4][(\eta^5\text{-}C_5Me_5)MoS_3(CuNCS)_3]\cdot$DMF ($3.09 \times 10^{-29}$ esu).[14d] However, their values are better than those found in C_{60} (7.5×10^{-34} esu) and C_{70} (1.3×10^{-33} esu),[24a,b] organometallic compounds such as group 10 metal alkynyl polymers (8.6×10^{-34} esu)[24c] and ferrocene (1.6×10^{-35} esu),[24d] and the films of TiOPc (*Pc* = phthalocyanine) complexes before and after annealing (1.04×10^{-33}∼5.35×10^{-34} esu).[24e,f] It is noted that when **1** was oxidized into **2**, the γ value of **2** is 11.7 times larger than that of **1** (1.07×10^{-32} esu),[14e] implying that existence of two $[Tp^*WS_3]$ units in **2** greatly enhances its NLO performance. The γ values of **3**−**7** are 2.10−2.49 times larger than that of their precursor **2**. Such an enhancement may be ascribed to be the incorporation of three or more Cu(I) atoms into each $[Tp^*WS_3]$ core of **2**. The γ values of **3**−**7** are 5.7−8.7 times larger than those of the $[Tp^*W(\mu_3\text{-}S)_3Cu_3]$-based single cubanelike clusters such as $[Et_4N]_2[Tp^*W(\mu_3\text{-}S)_3(CuNCS)_3(\mu_3\text{-Br})]$ (3.6×10^{-32} esu) and $\{[Et_4N][Tp^*W(\mu_3\text{-}S)_3(Cu\text{-}\mu\text{-SCN})_3(Cu\text{-}\mu_3\text{-NCS})]\}_n$ (4.6×10^{-32} esu), which may be due to existence of two $[Tp^*WS_3Cu_3]$ cluster cores in **3**−**7**. In addition, the γ values of **3**−**7** are 4.8−5.7 times larger than that of the thiocyanate-bridged double cubanelike W/Cu/S cluster $[Tp^*W(\mu_3\text{-}S)_3Cu_3(\mu\text{-NCS})_3(CuMeCN)]_2$ (5.46×10^{-32} esu).[14e] Such a difference may be ascribed to their different double cubanelike frameworks and also their peripheral groups in **3**−**7**.

CONCLUSIONS

In the work reported here, we have prepared a new W/S precursor $[(Tp^*WS_2)_2(\mu\text{-}S_2)]$ (**2**) by a redox reaction of **1** with AgSCN in MeCN. Reactions of **2** with excess CuX (X = Cl, Br, I) generated three neutral double cubanelike clusters **3**−**5** while those of **2** with CuX (X = Cl, Br) in the presence of Et_4NX (X = Cl, Br) generated two anionic double cubanelike clusters **6** and **7**, respectively. Compounds **3**−**7** display four types of unprecedented halide-bridged W/Cu/S double cubanelike structures. Two $[Tp^*W(\mu_3\text{-}S)_3Cu_3]$ cluster cores in **3** are connected via a μ_7-Cl bridge, two μ-Cl bridges, and a $[Cu(MeCN)(\mu\text{-Cl})_2]$ bridge. **4** contains one $[Tp^*W(\mu_3\text{-}S)_3Cu_3(MeCN)]^{2+}$ core and one $[Tp^*W(\mu_3\text{-}S)_3Cu_3Br]$ core connected by a μ_4-Br and two μ-Br bridges. **5** consists of two $[Tp^*W(\mu_3\text{-}S)_3Cu_3]$ cores linked by a linear $[(\mu\text{-I})_2Cu(\mu_3\text{-I})_2Cu(\mu\text{-I})_2]$ species. **6** or **7** possesses two $[Tp^*W(\mu_3\text{-}S)_3Cu_3X]$ cluster cores linked by a μ_4-X^- and two μ-X^- bridges (X = Cl, Br). The methodology reported here may provide an interesting route to metal sulfide clusters with double cubanelike structures. According to the results of the ESI mass spectra of **3**−**7**, these clusters might not be stable in solution and could not maintain their halide-bridged double cubanelike frameworks intact. Their halide bridges and CuX units were cleaved and their frameworks were broken into small cluster fragments under the mass conditions. In the cases of **4** and **5**, we could observe that some amount of clusters may still keep their main structure by losing several halide bridges and CuX units. The third-order NLO performance of **2** was greatly enhanced when CuX units were introduced to add onto the

[Tp*WS_3] units of **2** to form **3**−**7**. Compounds **3**−**7** showed good third-order NLO performances in solution. All these results demonstrate that **2** would be an excellent structural and NLO precursor for W/Cu/S cluster-based arrays. We are currently extending this work by studies on the formation of novel W/M/S double cubanelike clusters from reactions of **2** with copper(I), silver(I), and iron(II)/iron(III) salts.

EXPERIMENTAL SECTION

General Procedure. All manipulations were performed under an argon atmosphere using standard Schlenk-line techniques. Compound **1** was prepared according to the literature method.[15] All the solvents were predried over activated molecular sieves and refluxed over the appropriate drying agents under argon. Other chemicals and reagents were obtained from commercial sources and used as received. IR spectra were recorded on a Varian 1000 FT-IR spectrometer as KBr disks (4000−400 cm^{-1}). UV−vis spectra were measured on a Varian 50 UV−visible spectrophotometer. Elemental analyses for C, H, and N were performed on a Carlo-Erba CHNO-S microanalyzer. ^{1}H NMR spectra were recorded at ambient temperature on a Varian UNITYplus-400 spectrometer. The ^{1}H NMR chemical shifts were referenced to TMS in $CDCl_3$ or to the deuterated dimethyl sulfoxide (DMSO-d_6) signal. ESI mass spectra were performed on a DECAX-30000 LCQ Deca XP mass spectrometer using DMF as mobile phase.

Synthesis of [(Tp*WS_2)$_2$(μ-S_2)] (2). To a solution of **1** (500 mg, 0.7 mmol) in 15 mL of MeCN was added AgSCN (230 mg, 1.4 mmol). A large amount of black precipitate was developed within minutes, and the solution turned brown. After the mixture was stirred for 20 h at room temperature, the resulting solid was filtered and recrystallized in CH_2Cl_2 and filtered again. Diethyl ether was layered onto the filtrate to form dark green crystals of **2**·2CH_2Cl_2, which were collected, washed by Et_2O, and dried in vacuo to give pure **2**. Yield: 200 mg (49% based on W). Anal. Calcd. for $C_{30}H_{44}B_2N_{12}S_6W_2$: C, 31.21; H, 3.84; N, 14.56. Found: C, 31.49; H, 3.62; N, 14.37. IR (KBr disk): 2556 (w), 1543 (s), 1446 (m), 488 (m), 473 (s) cm^{-1}. UV−vis (MeCN/CH_2Cl_2, λ_{max}(nm (ε M^{-1} cm^{-1}))): 259 (39600). ^{1}H NMR (400 MHz, $CDCl_3$): δ 2.29 (s, 18H, CH_3 in Tp*), 2.80 (s, 18H, CH_3 in Tp*), 6.05 (s, 6H, CH in Tp*), the B−H proton was not located.

Synthesis of [{Tp*W(μ_3-S)$_3$$Cu_3$($\mu$-Cl)}$_2$Cu($\mu$-Cl)$_2$($\mu_7$-Cl)-(MeCN)] (3). To a dark green solution of **2** (23 mg, 0.02 mmol) in CH_2Cl_2 (1 mL) and $CHCl_3$ (1 mL) was added CuCl (9 mg, 0.09 mmol) in MeCN (1 mL). The resulting mixture was stirred at room temperature for 30 min and filtered. Et_2O (15 mL) was slowly layered onto the purple red filtrate to afford black blocks of **3**·CH_2Cl_2 four days later, which were collected by filtration, washed thoroughly with Et_2O, and dried in vacuo to give pure **3**. Yield: 33 mg (90% based on W). Anal. Calcd. for $C_{32}H_{47}B_2Cl_5Cu_7N_{13}S_6W_2$: C, 21.15; H, 2.61; N, 10.02. Found: C, 21.32; H, 2.79; N, 9.96. IR (KBr disk, cm^{-1}): 2565 (w), 1548 (s), 1449 (s), 480 (w), 405 (w) cm^{-1}. UV−vis (MeCN/CH_2Cl_2, λ_{max} (nm (ε M^{-1} cm^{-1}))): 325 (33900). ^{1}H NMR (400 MHz, $CDCl_3$): δ 2.09 (s, 3H, CH_3 in MeCN), δ 2.35 (s, 18H, CH_3 in Tp*), 2.87 (s, 18H, CH_3 in Tp*), 5.99 (s, 6H, CH in Tp*), the B−H proton was not located.

Synthesis of [{Tp*W(μ_3-S)$_3$$Cu_3$}$_2$Br($\mu$-Br)$_2$($\mu_4$-Br)(MeCN)] (4). Compound **4** was prepared in a manner similar to that described for **3**, by using **2** (23 mg, 0.02 mmol) in CH_2Cl_2 (1 mL) and $CHCl_3$ (1 mL) and CuBr (12 mg, 0.08 mmol) in MeCN (1 mL) as starting materials. Black block crystals of **4**·CH_2Cl_2·2$CHCl_3$ were collected, washed thoroughly with Et_2O, and dried in vacuo to give pure **4**. Yield: 32 mg (85% based on W). Anal. Calcd. for $C_{32}H_{47}B_2Br_4Cu_6N_{13}S_6W_2$: C, 20.27; H, 2.45; N, 9.60. Found: C, 20.59; H, 2.48; N, 9.32. IR (KBr disk, cm^{-1}): 2564 (w), 1547 (s), 1447 (s), 479 (w), 406 (w). UV−vis (MeCN/CH_2Cl_2, λ_{max} (nm (ε M^{-1} cm^{-1}))): 326 (16100). ^{1}H NMR (400 MHz, $CDCl_3$): δ 2.11 (s, 3H, CH_3 in MeCN), 2.39 (s, 18H, CH_3 in Tp*), 2.86 (s, 18H, CH_3 in Tp*), 6.14 (s, 6H, CH in Tp*), the B−H proton was not located.

Synthesis of [{Tp*W(μ_3-S)$_3$$Cu_3$}$_2${$Cu_2$($\mu$-I)$_4$($\mu_3$-I)$_2$}] (5). Compound **5** was prepared in a manner similar to that described for **3**, by using **2** (23 mg, 0.02 mmol) in CH_2Cl_2 (1 mL) and $CHCl_3$ (1 mL) and CuI (19 mg, 0.10 mmol) in MeCN (1 mL) as starting materials. Black block crystals of **5** were collected, washed thoroughly with Et_2O, and dried in vacuo to give pure **5**. Yield: 41 mg (84% based on W). Anal. Calcd. for $C_{30}H_{44}B_2I_6Cu_8N_{12}S_6W_2$: C, 14.86; H, 1.83; N, 6.93. Found: C, 14.95; H, 1.62; N, 6.79. IR (KBr disk, cm^{-1}): 2563 (w), 1549 (s), 1447 (s), 475 (w), 416 (w). UV−vis (MeCN/CH_2Cl_2, λ_{max} (nm (ε M^{-1} cm^{-1}))): 326 (38300). ^{1}H NMR (400 MHz, $CDCl_3$): δ 2.11 2.26 (s, 18H, CH_3 in Tp*), 2.79 (s, 18H, CH_3 in Tp*), 6.11 (s, 6H, CH in Tp*), the B−H proton was not located.

Synthesis of [Et_4N][{Tp*W(μ_3-S)$_3$$Cu_3$Cl}$_2$($\mu$-Cl)$_2$($\mu_4$-Cl)] (6). To a dark green solution of **2** (23 mg, 0.02 mmol) in CH_2Cl_2 (2 mL) was added CuCl (9 mg, 0.09 mmol) in MeCN (1 mL) in the presence of Et_4NCl (6 mg, 0.04 mmol). After being stirred at room temperature for 5 h, the resulting purple solution was filtered. Et_2O (15 mL) was carefully layered onto the filtrate to form black crystals of **6**·Et_2O in four days, which were collected by filtration, washed thoroughly with Et_2O, and dried in vacuo. Yield: 23 mg (63% based on W). Anal. Calcd. for $C_{38}H_{64}B_2Cl_5Cu_6N_{12}S_6W_2$: C, 24.95; H, 3.53; N, 9.19. Found: C, 24.68; H, 3.47; N, 9.33. IR (KBr disk, cm^{-1}): 2564 (w), 1548 (s), 1449 (s), 469 (w), 426 (w) cm^{-1}. UV−vis (MeCN/CH_2Cl_2, λ_{max} (nm (ε M^{-1} cm^{-1}))): 326 (29500). ^{1}H NMR (400 MHz, $CDCl_3$): δ 1.12−1.16 (t, 12H, CH_2CH_3), 2.38 (s, 18H, CH_3 in Tp*), 2.86 (s, 18H, CH_3 in Tp*), 3.20−3.29 (q, 8H, CH_2CH_3), 6.09 (s, 6H, CH in Tp*), the B−H proton was not located.

Synthesis of [Et_4N][{Tp*W(μ_3-S)$_3$$Cu_3$Br}$_2$($\mu$-Br)$_2$($\mu_4$-Br)] (7). Compound **7** was prepared in a manner similar to that described for **6**, by using **2** (23 mg, 0.02 mmol) in CH_2Cl_2 (2 mL), CuBr (12 mg, 0.08 mmol) in MeCN (1 mL) and Et_4NBr (8 mg, 0.04 mmol) as starting materials. Black crystals of **7**·1.5Et_2O were collected, washed thoroughly with Et_2O, and dried in vacuo. Yield: 27 mg (66% based on W). Anal. Calcd. for $C_{38}H_{64}B_2Br_5Cu_6N_{12}S_6W_2$: C, 22.25; H, 3.14; N, 8.19. Found: C, 22.59; H, 3.48; N, 8.32. IR (KBr disk, cm^{-1}): 2558 (w), 1543 (s), 1448 (s), 468 (w), 418 (w) cm^{-1}. UV−vis (MeCN, λ_{max} (nm (ε M^{-1} cm^{-1}))): 327 (21600). ^{1}H NMR (400 MHz, $CDCl_3$): δ 1.15−1.19 (t, 12H, CH_2CH_3), 2.36 (s, 18H, CH_3 in Tp*), 2.84 (s, 18H, CH_3 in Tp*), 3.14−3.21 (q, 8H, CH_2CH_3), 6.13 (s, 6H, CH in Tp*), the B−H proton was not located.

X-ray Structure Determination. Single crystals of **2**·2CH_2Cl_2, **3**·CH_2Cl_2, **4**·CH_2Cl_2·2$CHCl_3$, **5**, **6**·Et_2O, and **7**·1.5Et_2O were obtained directly from the above preparations. All measurements were made on a Rigaku Mercury CCD X-ray diffractometer by using graphite monochromated Mo Kα (λ = 0.71073 nm). Each crystal was mounted at the top of a glass fiber and cooled at 193 K in a stream of gaseous nitrogen. Cell parameters were refined by using the program CrystalClear (Rigaku and MSc, version 1.3, 2001) on all observed reflections. The collected data were reduced by using the program CrystalClear. The reflection data were also corrected for Lorentz and polarization effects.

The crystal structures of **2**·2CH_2Cl_2, **3**·CH_2Cl_2, **4**·CH_2Cl_2·2$CHCl_3$, **5**, **6**·Et_2O, and **7**·1.5Et_2O were solved by direct methods and refined on F^2 by full-matrix least-squares techniques with SHELXTL-97 program.[25] For **2**·2CH_2Cl_2, one CH_2Cl_2 solvent molecule was found to be disordered over two sites with 0.64/0.36 occupancy for Cl3−Cl4/Cl3A−Cl4A. For **4**·CH_2Cl_2·2$CHCl_3$, one $CHCl_3$ solvent molecule was split into three positions with an occupancy factor of 0.4/0.3/0.3 for Cl1−Cl3/Cl1A−Cl3A/Cl1B−Cl3B. For **5**, the single crystals we used always showed weak diffraction, especially at high angles, which made the final R value relatively high. For **6**·Et_2O and **7**·1.5Et_2O, each ethyl group of the Et_4N^+ cation was split into two sites, which were

dx.doi.org/10.1021/ic200147d |Inorg. Chem. 2011, 50, 4493–4502

Table 1. Crystallographic Data for $2\cdot 2CH_2Cl_2$, $3\cdot CH_2Cl_2$, $4\cdot CH_2Cl_2\cdot 2CHCl_3$, 5, $6\cdot Et_2O$, and $7\cdot 1.5Et_2O$

	$2\cdot 2CH_2Cl_2$	$3\cdot CH_2Cl_2$	$4\cdot CH_2Cl_2\cdot 2CHCl_3$	5	$6\cdot Et_2O$	$7\cdot 1.5Et_2O$
chemical formula	$C_{32}H_{48}B_2Cl_4N_{12}S_6W_2$	$C_{33}H_{49}B_2Cl_7Cu_7N_{13}S_6W_2$	$C_{35}H_{51}B_2Cl_8Br_4Cu_6N_{13}S_6W_2$	$C_{30}H_{44}B_2Cu_8I_6N_{12}S_6W_2$	$C_{42}H_{74}B_2Cl_5Cu_6N_{13}OS_6W_2$	$C_{44}H_{79}B_2Br_5Cu_6N_{13}O_{1.5}S_6W_2$
fw	1496.32	753.18	848.25	2424.29	1917.31	2176.67
cryst. syst.	monoclinic	orthorhombic	triclinic	triclinic	orthorhombic	orthorhombic
space group	$P2_1/c$	*Pnma*	$P\bar{1}$	$P\bar{1}$	*Pnma*	*Pnma*
a (Å)	20.297(4)	25.093(5)	11.557(2)	10.737(2)	21.152(4)	21.702(4)
b (Å)	14.392(3)	23.399(5)	13.558(3)	11.346(2)	24.156(5)	24.328(5)
c (Å)	16.935(3)	9.798(2)	22.986(5)	13.669(3)	15.478(3)	15.580(3)
α (deg)	94.37(3)			65.96(3)		
β (deg)	107.63(3)	103.90(3)		69.89(3)		
γ (deg)	111.54(3)			79.80(3)		
V (Å^3)	4714.5(16)	5753(2)	3197.7(15)	1426.7(6)	7909(3)	8226(3)
Z	2	4	2	1	4	4
T/K	223(2)	223(2)	223(2)	223(2)	223(2)	223(2)
D_{calcd} (g cm^{-3})	1.866	2.197	2.305	2.821	1.610	1.758
λ(Mo Kα) (Å)	0.71073	0.71073	0.71073	0.71073	0.71073	0.71073
μ (cm^{-1})	54.09	70.98	86.06	104.31	48.40	69.22
$2\theta_{max}$ (deg)	55.0	55.0	50.0	50.0	55.0	50.0
no. of reflns collected	26819	31544	26675	10230	40418	29006
no. of unique reflns	10701 (R_{int} = 0.0595)	6751 (R_{int} = 0.0477)	11172 (R_{int} = 0.0668)	4801 (R_{int} = 0.0954)	8981 (R_{int} = 0.0355)	7196 (R_{int} = 0.0450)
no. of obsd. reflns	8088 ($I > 2.00\sigma(I)$)	6128 ($I > 2.00\sigma(I)$)	8854 ($I > 2.00\sigma(I)$)	4196 ($I > 2.00\sigma(I)$)	8149 ($I > 2.00\sigma(I)$)	6308 ($I > 2.00\sigma(I)$)
no. of variables	544	334	696	304	393	433
R^a	0.0659	0.0473	0.0517	0.1327	0.0503	0.0489
wR^b	0.1219	0.1161	0.1239	0.3457	0.1399	0.1376
GOF^c	1.149	1.140	1.023	1.183	1.184	1.162

$^a R = \Sigma||F_o| - |F_c||/\Sigma|F_o|$. $^b wR = \{\Sigma w(F_o^2 - F_c^2)^2/\Sigma w(F_o^2)^2\}^{1/2}$. ^{c} GOF = $\{\Sigma w(F_o^2 - F_c^2)^2/(n-p)\}^{1/2}$, where *n* = number of reflections and *p* = total numbers of parameters refined.

centrosymmetric with respect to N7, with equal occupancy for C16−C23/C16A−C23A (symmetry code for **6**: A: $-x+1/2, -y+3/2, z+3/2$; symmetry code for **7**: A: $-x+3/2, -y+1/2, z+3/2$). In the case of $6\cdot Et_2O$ and $7\cdot 1.5Et_2O$, when crystals were taken out of their mother liquor, rapid evaporation of the Et_2O solvent molecules in the crystals were observed, which left a relatively large solvent accessible void (638 Å^3 for **6** and 407 Å^3 for **7**). For $2\cdot 2CH_2Cl_2$, $3\cdot CH_2Cl_2$, $4\cdot CH_2Cl_2\cdot 2CHCl_3$, **5**, $6\cdot Et_2O$, and $7\cdot 1.5Et_2O$, all non-hydrogen atoms, except for those of the $CHCl_3$ molecule in $4\cdot CH_2Cl_2\cdot 2CHCl_3$, one Et_2O molecule in $6\cdot Et_2O$, and one Et_2O molecule in $7\cdot 1.5Et_2O$, were refined anisotropically. Each hydrogen atom at the B atom of $4\cdot CH_2Cl_2\cdot 2CHCl_3$, $6\cdot Et_2O$, and $7\cdot 1.5Et_2O$ were located from Fourier maps. The hydrogen atom at C33 of the $CHCl_3$ molecule in **4** was not located. Other hydrogen atoms were placed in geometrically idealized positions (C−H = 0.98 Å, with $U_{iso}(H) = 1.5U_{eq}(C)$ for methyl groups; C−H = 0.99 Å, with $U_{iso}(H) = 1.2U_{eq}(C)$ for methylene groups; C−H = 0.95 Å, with $U_{iso}(H) = 1.2U_{eq}(C)$ for aromatic rings) and constrained to ride on their parent atoms. A summary of the key crystallographic information for $2\cdot 2CH_2Cl_2$, $3\cdot CH_2Cl_2$, $4\cdot CH_2Cl_2\cdot 2CHCl_3$, **5**, $6\cdot Et_2O$, and $7\cdot 1.5Et_2O$ is listed in Table 1.

Third-Order Nonlinear Optical (NLO) Measurements of 2−7. The solutions of **2**−**7** (5.0×10^{-5} M) in CH_2Cl_2/MeCN were placed in a 1.5 mm quartz cuvette for the third-order NLO measurements. These six compounds were stable toward air and laser light under experimental conditions. As a reference, the optical nonlinearity of the standard sample CS_2 was also observed. The third-order NLO properties were measured using femtosecond DFWM technique with a Ti: Sapphire laser (Spectra-physics Spitfire Amplifier). The pulse width was determined to be 80 fs on a SSA25 autocorrelator. The operating wavelength was centered at 800 nm. The repetition rate of the pulses was 1 kHz. During the measurement the laser was very stable (rms <0.1%). The input beam was split into two beams k_1 and k_2 with nearly equal energy by use of a beam splitter (BS) and then focused on a plot of the sample. The beam k_2 passed through a delay line derived by a stepping motor in order that the optical path length difference between the k_2 and k_1 beams could be adjusted during the measurement. The angle between the beams k_1 and k_2 were about 5°. When k_1 and k_2 were overlapped spatially in the sample, the generated signal beam k_3 passed through an aperture, recorded by a photodiode and then analyzed by a lock-in amplifier and computer.

■ ASSOCIATED CONTENT

Supporting Information. Crystallographic data of $2\cdot 2CH_2Cl_2$, $3\cdot CH_2Cl_2$, $4\cdot CH_2Cl_2\cdot 2CHCl_3$, **5**, $6\cdot Et_2O$, and $7\cdot 1.5Et_2O$ (CIF format), ESI mass spectra for **3**−**7** and DFWM signal for **3**−**7** in PDF format. This material is available free of charge via the Internet at http://pubs.acs.org.

■ AUTHOR INFORMATION

Corresponding Author
*E-mail: jplang@suda.edu.cn.

■ ACKNOWLEDGMENT

This work was financially supported by the National Natural Science Foundation of China (20525101, 20871088, and 90922018), the Nature Science Key Basic Research of Jiangsu Province for Higher

Education (09KJA150002), the Specialized Research Fund for the Doctoral Program of higher Education of Ministry of Education (20093201110017), the State Key Laboratory of Organometallic Chemistry of Shanghai Institute of Organic Chemistry (08-25), the Priority Academic Program Development of Jiangsu Higher Education Institutions, the Qin-Lan and the "333" Projects of Jiangsu Province, the "SooChow Scholar" Program and Program for Innovative Research Team of Suzhou University.

REFERENCES

(1) (a) Chan, M. K.; Kim, J.; Rees, D. C. *Science* **1993**, *260*, 792. (b) Peters, J. W.; Stowell, M. H. B.; Soltis, S. M.; Finnegan, M. G.; Johnson, M. K.; Rees, D. C. *Biochemistry* **1997**, *36*, 1181. (c) Mayer, S. M.; Lawson, D. M.; Gormal, C. A.; Roe, S. M.; Smith, B. E. *J. Mol. Biol.* **1999**, *292*, 871.

(2) (a) Chakrabarti, M.; Deng, L.; Holm, R. H.; Münck, E.; Bominaar, E. L. *Inorg. Chem.* **2010**, *49*, 1647. (b) Takei, I.; Kobayashi, K.; Dohki, K.; Hidai, M. *Inorg. Chem.* **2007**, *46*, 1045. (c) Malinak, S. M.; Coucouvanis, D. *Prog. Inorg. Chem.* **2001**, *49*, 599.

(3) Li, Z.; Du, S. W.; Wu, X. T. *Dalton Trans.* **2004**, 2438.

(4) (a) Rejai, Z.; Lühmann, H.; Näther, C.; Kremer, R. K.; Bensch, W. *Inorg. Chem.* **2010**, *49*, 1651. (b) Scott, T. A.; Holm, R. H. *Inorg. Chem.* **2008**, *47*, 3426.

(5) (a) Wolff, T. E.; Power, P. P.; Frankel, R. B.; Holm, R. H. *J. Am. Chem. Soc.* **1980**, *102*, 4694. (b) Christou, G.; Garner, C. D. *J. Chem. Soc., Dalton Trans.* **1980**, 2354. (c) Herbst, K.; Monari, M.; Brorson, M. *Inorg. Chem.* **2002**, *41*, 1336.

(6) (a) Ogo, S.; Suzuki, T.; Ozawa, Y.; Isobe, K. *Inorg. Chem.* **1996**, *35*, 6093. (b) Lang, J. P.; Kawaguchi, H.; Ohnishi, S.; Tatsumi, K. *Chem. Commun.* **1997**, 405. (c) Beheshti, A.; Clegg, W.; Hyvadi, R.; Hekmat, H. F. *Polyhedron* **2002**, *21*, 1547. (d) Lang, J. P.; Xu, Q. F.; Chen, Z. N.; Abrahams, B. F. *J. Am. Chem. Soc.* **2003**, *125*, 12682.

(7) (a) Du, S. W.; Zhu, N. Y.; Chen, P. C.; Wu, X. T. *Polyhedron* **1992**, *11*, 2495. (b) Xu, J. Q.; Zhang, X. G.; Cai, H.; Hu, N. H.; Wei, C. P.; Yang, G. Y.; Wang, T. G. *Chem. Commun.* **1996**, 757. (c) Ren, Z. G.; Li, H. X.; Li, L. L.; Zhang, Y.; Lang, J. P.; Yang, J. Y.; Song, Y. L. *J. Organomet. Chem.* **2007**, *692*, 2205. (d) Wei, Z. H.; Li, H. X.; Cheng, M. L.; Tang, X. Y.; Chen, Y.; Zhang, Y.; Lang, J. P. *Inorg. Chem.* **2009**, *48*, 2808.

(8) (a) Lang, J. P.; Kawaguchi, H.; Ohnishi, S.; Tatsumi, K. *Inorg. Chim. Acta* **1998**, *283*, 136. (b) Arliguie, T.; Thuéry, P.; Le Floch, P.; Mézailles, N.; Ephritikhine, M. *Polyhedron* **2009**, *28*, 1578. (c) Huang, Y. J.; Song, Y. L.; Chen, Y.; Li, H. X.; Zhang, Y.; Lang, J. P. *Dalton Trans.* **2009**, 1411.

(9) (a) Sakane, G.; Yao, Y. G.; Shibahara, T. *Inorg. Chim. Acta* **1994**, *216*, 13. (b) Huang, J.; Mukerjee, S.; Segal, B. M.; Akashi, H.; Zhou, J.; Holm, R. H. *J. Am. Chem. Soc.* **1997**, *119*, 8662. (c) Huang, J.; Holm, R. H. *Inorg. Chem.* **1998**, *37*, 2247. (d) Shinozaki, A.; Seino, H.; Hidai, M.; Mizobe, Y. *Organometallics* **2003**, *22*, 4636. (e) Lee, S. C.; Holm, R. H. *Chem. Rev.* **2004**, *104*, 1135.

(10) (a) Chadwick, S.; Englich, U.; Ruhlandt-Senge, K. *Organometallics* **1997**, *16*, 5792. (b) Freedman, D.; Melman, J. H.; Emge, T. J.; Brennan, J. G. *Inorg. Chem.* **1998**, *37*, 4162. (c) Kure, B.; Ogo, S.; Inoki, D.; Nakai, H.; Isobe, K.; Fukuzumi, S. *J. Am. Chem. Soc.* **2005**, *127*, 14366.

(11) (a) Jones, W. D.; Chin, R. M. *J. Am. Chem. Soc.* **1994**, *116*, 198. (b) Kuwata, S.; Hidai, M. *Coord. Chem. Rev.* **2001**, *213*, 211. (c) Feliz, M.; Llusar, R.; Uriel, S.; Vicent, C.; Brorson, M.; Herbst, K. *Polyhedron* **2005**, *10*, 1212.

(12) (a) Zhang, Q. C.; Chung, I.; Jang, J. I.; Ketterson, J. B.; Kanatzidis, M. G. *J. Am. Chem. Soc.* **2009**, *131*, 9896. (b) Ren, Z. G.; Yang, J. Y.; Song, Y. L.; Li, N. Y.; Li, H. X.; Chen, Y.; Zhang, Y.; Lang, J. P. *Dalton Trans.* **2009**, 2578. (c) Zhang, Q. C.; Chung, I.; Jang, J. I.; Ketterson, J. B.; Kanatzidis, M. G. *J. Am. Chem. Soc.* **2009**, *131*, 9896.

(13) (a) Lang, J. P.; Tatsumi, K. *Inorg. Chem.* **1998**, *37*, 6308. (b) Lang, J. P.; Tatsumi, K. *J. Organomet. Chem.* **1999**, *579*, 332. (c) Zhang, W. H.; Liu, D.; Li, H. X.; Ren, Z. G.; Zhang, Y.; Lang, J. P. *Cryst. Growth. Des.* **2010**, *10*, 3.

(14) (a) Shi., S.; Ji, W.; Tang, S. H. *J. Am. Chem. Soc.* **1994**, *116*, 3615. (b) Shi, S.; Ji, W.; Xie, W.; Chong, T. C.; Zheng, H. C.; Lang, J. P.; Xin, X. Q. *Mater. Chem. Phys.* **1995**, *39*, 298. (c) Zhang, W. H.; Chen, J. X.; Li, H. X.; Wu, B.; Tang, X. Y.; Ren, Z. G.; Zhang, Y.; Lang, J. P.; Sun, Z. R. *J. Organomet. Chem.* **2005**, *690*, 394. (d) Zhang, W. H.; Song, Y. L.; Ren, Z. G.; Li, H. X.; Li, L. L.; Zhang, Y.; Lang, J. P. *Inorg. Chem.* **2007**, *46*, 6647. (e) Wang, J.; Sun, Z. R.; Deng, L.; Wei, Z. H.; Zhang, W. H.; Zhang, Y.; Lang, J. P. *Inorg. Chem.* **2007**, *46*, 11381. (f) Wei, Z. H.; Li, H. X.; Ren, Z. G.; Lang, J. P.; Zhang, Y.; Sun, Z. R. *Dalton Trans* **2009**, 3425.

(15) (a) Seino, H.; Arai, Y.; Iwata, N.; Nagao, S.; Mizobe, Y.; Hidai, M. *Inorg. Chem.* **2001**, *40*, 1677. (b) Müller, A.; Diemann, E.; Jostes, R.; Bögge, H. *Angew. Chem., Int. Ed.* **1981**, *20*, 934. (c) Ansari, M. A.; Ibers, J. A. *Coord. Chem. Rev.* **1990**, *100*, 223. (d) Jeannin, Y.; Sèheresse, F.; Bernés, S.; Robert, F. *Inorg. Chim. Acta* **1992**, *198*−*200*, 493.(e) Wu, X. T. *Inorganic Assembly Chemistry*; Science Press and Science Press USA Inc.: Beijing, 2004; p 1. (f) Hou, H. W.; Xin, X. Q.; Shi, S. *Coord. Chem. Rev.* **1996**, *153*, 25. (g) Niu, Y. Y.; Zheng, H. G.; Xin, X. Q. *Coord. Chem. Rev.* **2004**, *248*, 169.(h) Shi, S. In *Optoelectronic Properties of Inorganic Compounds*; Roundhill, D. M., Fackler, J. P., Jr., Eds.; Plenum Press: New York, 1998; p 55. (i) Coe, B. J. In *Comprehensive Coordination Chemistry II*; McCleverty, J. A., Meyer, T. J., Eds.; Elsevier Pergamon: Oxford, U.K., 2004; Vol. 9, p 621. (j) Zhang, C.; Song, Y. L.; Wang, X. *Coord. Chem. Rev.* **2007**, *251*, 111.

(16) (a) Horikoshi, R.; Mochida, T.; Moriyama, H. *Inorg. Chem.* **2002**, *41*, 3017. (b) Caradoc-Davies, P. L.; Hanton, L. R. *Dalton Trans.* **2003**, 1754. (c) Humphrey, S. M.; Mole, R. A.; Rawson, J. M.; Wood, P. T. *Dalton Trans.* **2004**, 1670. (d) Wang, J.; Zheng, S. L.; Hu, S.; Zhang, Y. H.; Tong, M. L. *Inorg. Chem.* **2007**, *46*, 795. (e) Chen, Y.; Wang, Z. O.; Ren, Z. G.; Li, H. X.; Li, D. X.; Liu, D.; Zhang, Y.; Lang, J. P. *Cryst. Growth. Des.* **2009**, *9*, 4963.

(17) Capps, K. B.; Whitener, G. D.; Bauer, A.; Abboud, K. A.; Wasser, I. M.; Vollhardt, K. P. C.; Hoff, C. D. *Inorg. Chem.* **2002**, *41*, 3212.

(18) Yu, H.; Zhang, W. H.; Cao, X. Q.; Chen, Y.; Ren, Z. G.; Lang, J. P. *Chin. J. Inorg. Chem.* **2006**, *22*, 187.

(19) (a) Hammond, R. P.; Cavaluzzi, M.; Haushalter, R. C.; Zubieta, J. A. *Inorg. Chem.* **1999**, *38*, 1288. (b) Pronold, M.; Scheer, M.; Wachter, J.; Zabel, M. *Inorg. Chem.* **2007**, *46*, 1396. (c) Domasevitch, K. V.; Rusanova, J. A.; Vassilyeva, O. Y.; Kokozay, V. N.; Squattrito, P. J.; Sieler, J.; Raithby, P. R. *J. Chem. Soc., Dalton Trans.* **1999**, 3087. (d) Liaw, B. J.; Lobana, T. S.; Lin, Y. W.; Wang, J. C.; Liu, C. W. *Inorg. Chem.* **2005**, *44*, 9921.

(20) (a) Li, L. K.; Chen, B. Y.; Song, Y. L.; Li, G.; Hou, H. W.; Fan, Y. T.; Mi, L. W. *Inorg. Chim. Acta* **2003**, *344*, 95. (b) Orezyk, M. E.; Samoc, M.; Swiatkiewicz, J.; Prasad, P. N. *J. Chem. Phys.* **1993**, *98*, 2524. (c) Jenekhe, S. A.; Lo, S. K.; Flom, S. R. *Appl. Phys. Lett.* **1989**, *54*, 2524. (d) Mandal, B. K.; Bihari, B.; Sinha, A. K.; Kamath, M.; Chen, L. *Appl. Phys. Lett.* **1995**, *66*, 932.

(21) (a) Swiatkiewicz, J.; Prasad, P. N.; Reinhardt, B. A. *Opt. Commun.* **1998**, *157*, 135. (b) Kim, O. K.; Lee, K. S.; Woo, H. Y.; Kim, K. S.; He, G. S.; Swiatkiewicz, J.; Prasad, P. N. *Chem. Mater.* **2000**, *12*, 284.

(22) (a) Zhan, X. W.; Liu, Y. Q.; Zhu, D. B.; Liu, X. C.; Xu, G.; Ye, P. X. *Chem. Phy. Lett.* **2002**, *362*, 165. (b) Zhan, X. W.; Yang, M. J.; Xu, G.; Liu, X. C.; Ye, P. X. *Macromol. Rapid Commun.* **2001**, *22*, 358. (c) Zhan, X. W.; Liu, Y. Q.; Zhu, D. B.; Huang, W. T.; Gong, Q. H. *J. Phys. Chem. B* **2002**, *106*, 1884. (d) Rao, D. V. G. L. N.; Aranda, F. J.; Roach, J. F.; Remy, D. E. *Appl. Phys. Lett.* **1991**, *58*, 1241.

(23) (a) Zhang, C.; Song, Y. L.; Xu, Y.; Fun, H. K.; Fang, G. Y.; Wang, Y. X.; Xin, X. Q. *J. Chem. Soc., Dalton Trans.* **2000**, 2823. (b) Zhang, C.; Song, Y. L.; Kühn, F. E.; Xu, Y.; Xin, X. Q.; Fun, H. K.; Herrmann, W. A. *Eur. J. Inorg. Chem.* **2002**, 55. (c) Wu, B.; Zhang, W. H.; Li, H. X.; Ren., Z. G.; Lang, J. P.; Zhang, Y.; Song, Y. L. *J. Mol. Struct.* **2007**, *829*, 128.

(24) (a) Chen, Z. M.; Xia, C. H.; Wu, Y. Q.; Zuo, X.; Song, Y. L. *Inorg. Chem. Commun.* **2006**, *9*, 187. (b) Hou, H. W.; Liang, B.;

Xin, X. Q.; Yu, K. B.; Ge, P.; Shi, S. *J. Chem. Soc., Faraday Trans.* **1996**, *92*, 2343. (c) Blau, W. J.; Byrne, H. J.; Cardin, D. J.; Davey, A. P. *J. Mater. Chem.* **1991**, *1*, 245. (d) Guha, S.; Frazier, C. C.; Porter, P. L.; Kang, K.; Finberg, S. E. *Opt. Lett.* **1989**, *14*, 952. (e) Hosoda, M.; Wada, T.; Yamada, A.; Garito, A. F.; Sasabe, H. *Mater. Res. Soc. Symp. Proc.* **1990**, *175*, 89. (f) Hosoda, M.; Wada, T.; Yamada, A.; Garito, A. F. *Jpn. J. Appl. Phys.* **1991**, *30*, L1486.

(25) (a) Sheldrick, G. M. *SHELXS-97, Program for solution of crystal structures*; University of Göttingen: Göttingen, Germany, 1997. (b) Sheldrick, G. M. *SHELXL-97, Program for refinement of crystal structures*; University of Göttingen: Göttingen, Germany, 1997.